

21

22

Abstract

23

24

25

26

27

28

29

30

31

32

33

34

35

36

37

38

39

40

41

42

Keywords: resting state functional connectivity; fNIRS; early childhood; Freeplay;

43

44

45 **Introduction**

46

47 Brain function arises from a concerted effort of various regions working together in what can be
48 characterized as networks. Research in the past few decades has focused on properties of these networks
49 and patterns of connectivity that support cognitive functions [1-3]. Resting state networks (RSNs) --
50 networks of regions showing temporal correlation of low-frequency fluctuations (functional connections)
51 in subjects not performing any task [4] -- can reflect underlying functional organization of the brain.

52 Discovery of resting state functional connectivity (RSFC) and its link to function [5-8] has
53 widened the door to investigating mechanisms of cognitive function by providing some advantages over
54 task-based studies: 1) whereas measuring functional connectivity during task provides us with the
55 connectivity of only those regions specifically involved in the task, measurement during resting state can
56 provide connectivity information simultaneously among many regions; 2) certain populations (e.g.,
57 clinical populations) or cognitive functions (e.g., motor) that are difficult to engage with specific tasks in
58 the scanner, can be just as well studied in resting state. For these reasons, resting state measurement has
59 become a standard paradigm for studying functional connectivity in human adults.

60

61 **Measuring RSN development**

62

63 RSN research in infants and adults presents a clear developmental trend: whereas 10-20 RSNs
64 have been identified in adults, only about 5 of these networks are found in infants, the rest likely
65 developing throughout childhood [9,10]. This suggests that the functional architecture of the brain may
66 be undergoing dramatic development and restructuring in these intermediate years to create many of these
67 networks that emerge prominently by adulthood. *Patterns* of connectivity also change over development

68 -- a number of studies have shown that children display more diffuse functional connectivity patterns and
69 increased connectivity with adjacent regions, while adults show more focal connectivity patterns and
70 increased connectivity between distant regions [11,12]. This simultaneous increase in both segregation
71 (pruning short-range connections) and integration (strengthening long-range connections) of brain regions
72 over development likely reflects a transition from organization around spatial proximity to organization
73 around higher-order function [12]. Finally, aberrant connectivity in RSNs have been associated with a
74 variety of psychopathologies from affective disorders such as depression, to diseases of cognitive function
75 such as Alzheimer's disease, to neurodevelopmental disorders such as autism or ADHD (for review, see
76 [10]), suggesting that RSN development may be integral to healthy brain and cognitive development.
77 Together, these findings highlight the need for studying RSNs over the time course of development and
78 especially in early childhood, when perhaps the most change is occurring in some brain networks.

79 However, studying RSNs in children has been challenging, mainly for two reasons. First,
80 traditional neuroimaging tools (e.g., functional MRI (fMRI), electroencephalography (EEG), or
81 magnetoencephalography (MEG)) are difficult to utilize with awake children [13,14]. Second, the
82 standard procedure for measuring resting state connectivity -- to sit still for a period of time -- proves to
83 be a difficult task for children, and some methods previously employed to increase compliance in children
84 during resting state measurement, such as movie or video-watching, have been shown to significantly alter
85 resting state in adult participants [15]. Consequently, resting state studies in children and especially in
86 young (3-5 years/pre-school aged) children have been limited [16]. The current study uses functional near-
87 infrared spectroscopy (fNIRS) which provides an appropriate solution to child neuroimaging challenges
88 and introduces a new paradigm called Freeplay to address the difficulty of employing an appropriate
89 "task" for resting state measurement – the combination provides a simple and efficient paradigm to
90 improve participant compliance and quality RSFC measurement (of surface regions) in children. By
91 reconstructing characteristic features of RSFC, we demonstrate the feasibility of this fNIRS-Freeplay set-

92 up for studying resting state connectivity in preschool and early school-aged children. We also study the
93 test-retest reliability of the paradigm under a number of measures, showing that consistent results can be
94 derived across multiple scans, at both individual and group levels. Some multi-session test-retest reliability
95 studies for RSFC measurement methods exist for adults and older children in fMRI, as well as for adults
96 in fNIRS, but not for children in fNIRS [17-20].

97

98 **fNIRS with young children**

99

100 Traditionally studied with fMRI, and to a lesser degree with EEG/MEG, RSNs have been studied
101 primarily in adult and sleeping infant populations, but relatively rarely in child populations, as these
102 imaging techniques are challenging to use with awake children [21]. For example, a major difficulty is the
103 sensitivity of these modalities to movement artifacts combined with children's difficulty remaining still
104 for extended periods of time, which can systematically bias functional connectivity measures [22]. In a
105 previous study on the feasibility of fMRI measurement in children, Byars et al. [13] reported a 47%
106 success rate with children between the ages of 5 and 6, under a relatively generous definition of "success"
107 as 'completing at least one of four fMRI tasks and an anatomical reference scan' [14] (p. 2). Moreover,
108 another more recent study of fMRI feasibility with children and adolescents showed that clinical groups
109 scanned even less successfully than typically developing controls [14].

110 fNIRS is a relatively recent light-based neuroimaging method that overcomes many of the
111 challenges with obtaining brain activity measures in child populations. In fNIRS, near-infrared light is
112 used to obtain an estimate of changes in both oxygenated and deoxygenated hemoglobin concentrations
113 in a region of the brain. Thus, like fMRI, fNIRS gives an indirect measure of neural activity based on
114 blood oxygenation levels. Compared to fMRI or EEG, fNIRS is robust to and unrestrictive of motion,
115 comfortable, quick to set up, and cost effective (see [23] for comparison of techniques). These factors

116 make it especially appropriate for use with children. The main limitation of fNIRS in the context of
117 studying RSFC is that measurement is limited to regions near the surface of the brain (<17 mm of brain
118 tissue deep). For researchers interested in studying RSFC among surface regions of the brain, this is a
119 viable neuro-measurement tool. Our study, as discussed below, measures from the surface of the prefrontal
120 cortex.

121

122 **Freeplay in a fNIRS recording set-up can overcome challenges in behavioral methods**

123 Resting state studies have mainly recorded from adults instructed to remain still for a period of
124 time [24]. Some RSFC studies are conducted in infants during sleep [25]. Unfortunately, neither recording
125 situation is practical for young children; children often have great difficulty remaining quietly still for an
126 extended time, and unlike infants, children are far less susceptible to maintaining sleep in the scanner.
127 Moreover, it is not clear that sleep is a good approximation of resting state, as it exhibits its own distinctive
128 functional connectivity patterns [26-29]. For such reasons, resting state-fMRI studies that are run with
129 children frequently involve extensive and costly effort in pre-training children in “mock” scanner
130 environments to help reduce motion artifacts and improve participant compliance. In spite of this pre-
131 training, unwieldy proportions of scans (e.g., ranging from as little as 18% to as much as 53% in children
132 aged 4-6) are discarded due to movement artifacts contaminating the signal [30,31].

133 To mitigate this, many resting state-fMRI studies with children and patient populations have used
134 motion picture stimuli, with or without audio, to help engage participants in the fMRI scanner. These have
135 had some success in improving participant compliance (e.g., reduced participant motion and reduced
136 frequency of falling asleep) [32,33]. However, viewing movie clips have been found to significantly alter
137 resting state in adult participants [15]. Furthermore, viewing movie clips may engage task-specific
138 networks, such as those involved in language or audition. In fact, movies are sometimes used in studies
139 as stimuli or tasks [34], or have specifically been reported to induce different connectivity patterns

140 compared to rest (e.g., early visual network decreased its connectivity with dorsal attention network and
141 increased its connectivity with the default mode network as well as the fronto-parietal network, during
142 movie watching [33]. These findings bring into question the validity of using movies for studying “resting
143 state” -functional connectivities and -networks in particular. However, movie or video-watching still
144 remains the most feasible method by which to record RSFC from children in an fMRI setting (with varying
145 success depending on where the movie lies in the spectrum from too engaging to not engaging enough).

146 Because fNIRS recording set-up is quiet, comfortable to wear, and unrestrictive compared to the
147 fMRI environment, a less engaging set-up for aiding compliance can be sufficient. Our study proposes an
148 experimental paradigm called Freeplay that may closely approximate resting state, and which takes
149 advantage of the spatially unrestrictive nature of an fNIRS recording situation. In this “task”, participants
150 are seated at a table, presented with a set of simple toys (e.g., wooden blocks, small plastic animals) and
151 asked to quietly play for a few minutes. The premise is that children can naturally comply much more
152 easily with sitting still and quietly for a period of time when presented with even simple and unengaging
153 toys. In addition, the fNIRS possible sampling rate is much greater than that of fMRI, thus requiring less
154 recording time overall. Due to the simple nature of the toys, Freeplay is expected to induce quiet boredom,
155 a state we expect may closely approximate resting state. Additionally, the unconstrained nature of this set-
156 up naturally mirrors the “at rest” eyes-open set-up for adults in which adults sit open-endedly for a period
157 of time without any specific task, and in the same way, allows natural individual variation to be present.
158 Allowing natural variability is important as it allows researchers to be more confident that connectivity
159 patterns consistent across many participants are generalizable and not arising from task-specific or stimuli-
160 specific states.

161

162 Since measuring RSFC in children relies on using *approximations* of the resting state task (e.g.,
163 movie watching, silent rest), it is important to also develop multiple such approximations, to combat the

164 task impurity problem. Freeplay contributes as one method for approximating resting state. Moreover,
165 Freeplay avoids several biases that are inherent in some previous methods. For example, relatively
166 engaging or externally-guided stimuli, such as movie clips or screensavers, potentially compromise the
167 unrestrained and non-externally-directed nature of thinking that is characteristic of true resting state. They
168 may also potentially engage functional networks differently from rest (e.g., naturalistic movie viewing has
169 been shown to alter connectivity patterns among certain networks compared to rest) [33]. In contrast,
170 Freeplay's undirected or internally-/self- guided nature may more closely mirror the state of adults in
171 resting state. Additionally, in contrast to other proposed methods that utilize identical or similar visual
172 stimuli sequences across participants (movies, screensaver-type stimuli, e.g., Inscapes), Freeplay lacks
173 any time-locking events that could introduce systematic biases when aggregating data across subjects and
174 artificially inflate across-subject consistencies [35].

175

176

177 **Prefrontal Cortex**

178

179 The prefrontal cortex (PFC) houses major components of such RSNs as the central executive
180 network (CEN) and default mode network (DMN). Its development, from infancy through adulthood, is
181 prominently linked to the development of executive function (EF) [36], a collective system of basic
182 cognitive processes that includes inhibition, working memory, and cognitive flexibility, and supports
183 higher-order processes such as planning and problem solving [37,38]. PFC's protracted development
184 make it an especially interesting region to study over age, including in early development. Aberrant
185 functional connections within the PFC have also been associated with ADHD symptoms and impaired
186 inhibitory and attentional control, implicating its important role in health executive function development
187 [39]. Additional advantages of measuring PFC with fNIRS are its close proximity to the surface of the

188 skull and convenient placement under the forehead (which lacks hair, improving fNIRS signal quality).
189 Thus, we focused data collection on the PFC in this validation study.

190

191 **Current study**

192

193 This study aims to demonstrate feasibility of using fNIRS and Freeplay to measure RSFC in pre-
194 school-aged and early school-aged children. We present this paradigm as a potential means to address the
195 gap in research on RSFC in children, stemming from a lack of appropriate measurement and behavioral
196 tools for the population. This set-up is designed to place minimal restrictions on the participant, allow
197 sufficient data collection, and achieve relatively good signal-to-noise ratio (by minimizing sources of
198 noise introduced by the measurement tool as well as the participant). This study aims to establish
199 fundamental psychometric properties of the fNIRS-Freeplay paradigm, including construct validity, test-
200 retest reliability, and feasibility.

201

202 **Experiment 1: Comparison with traditional adult resting state**

203

204 We first investigated whether the fNIRS-Freeplay paradigm allows us to measure RSFC --
205 specifically, whether the paradigm exhibits construct validity. We did this in two ways. First, we asked
206 whether the fNIRS-Freeplay paradigm reproduces a characteristic feature of adult resting state
207 connectivity, namely strong connectivity between homologous (bilaterally symmetric) regions of the two
208 hemispheres [40,41]. Second, we studied the distinguishability of RSFC in adults in Freeplay and adults
209 in true resting state, in terms of the ability of machine learning classifiers to correctly classify instances of
210 each.

211 If adults “at rest” and in Freeplay show *similar* connectivity patterns and are difficult to distinguish

212 from each other, this would suggest that Freeplay may be a good approximation of resting state.
213 Confirming this hypothesis would help validate fNIRS-Freeplay as a paradigm for measuring RSFC in
214 adults, and a natural next step would be to apply this paradigm to measure RSFC in children. To begin
215 exploring this (and also to provide a control for our first similarity measure -- classification error between
216 adults in Freeplay and “at rest”), we additionally measured NIRS-Freeplay data in children, hypothesizing
217 that adults and children in Freeplay will show *different* connectivity patterns, consistent with research
218 suggesting significant development of RSFC from childhood into adulthood [9].

219

220 **Methods**

221 **Participants**

222

223 Participants were 13 undergraduates (aged 18-21) from Carnegie Mellon University (CMU) and
224 18 children (aged 3 to 8 years, $M_{\text{age}} = 4.8$, $Med_{\text{age}} = 4.3$) recruited from the community and the Children’s
225 School, a CMU-affiliated laboratory school. 17 children were included in the analysis after 1 exclusion
226 due to experimenter error. Adults participated in both the standard resting state task and the Freeplay task
227 within a single session. Task order was randomized. Children participated in Freeplay only.

228

229 **Standard Resting State Task**

230

231 Participants sat still and quietly at a desk with eyes open for 8 minutes. The scanning duration of
232 8 minutes sits comfortably over a 7-minute minimum reported to achieve accurate and stable RSFC from
233 fNIRS measurement in children (aged 6.9 to 8.21 years) in a recent study by Wang, Dong, and Niu testing
234 fNIRS RSFC test-retest reliability [42].

235

236 **Freeplay Set-up**

237

238 Participants sat quietly and freely played with a set of toys for about 8 minutes. Toys included:
239 lincoln logs, wooden nuts and bolts, plastic animal figurines, toy cars, and simple coloring pages (a flower,
240 turtle, duck, or fish). Toys were chosen to be simple and minimally engaging, to help induce quiet boredom,
241 a state that we expect may closely approximate resting state (See Figure 1, [right panel](#)).

242

243

244

245 **Fig. 1. Placement of NIRS probe.** The left picture displays NIRS probe strip placed over the forehead;
246 the right picture shows probe strip secured by scuba cap and the freeplay setup with simple toys.

247

248

249 **fNIRS Set-up**

250

251 Neural activity was recorded at 20 Hz using a continuous wave real-time fNIRS system (CW6,
252 Techen, Inc., Milford, MA, USA) with 4 light sources, each containing 690-nm (12 mW) and 830-nm (8
253 mW) laser light, and 8 detectors, to give oxy-hemoglobin and deoxy-hemoglobin measures in 10 channels
254 on the PFC (Figure 1, left panel). Sensors were arranged in a layout as depicted in Figure 2. The distance
255 between light sources and detectors were between 2.8 and 3 cm. Sensors were snapped into a cap strip
256 built from foam sheet and plastic mesh, and connected to the fNIRS system via optic fibers. For each
257 participant, the cap strip was positioned on the head, centered on position FpZ according to the
258 international 10-20 coordinate system standard, extending over the Brodmann area 10 (anterior PFC) and
259 area 46 (dorsolateral PFC) bilaterally. The strip was secured to the head using a neoprene scuba cap
260 (pictured in Figure 1), to prevent probe from slipping as well as to cover the probe to prevent ambient

261 light from reaching the sensors. The participant sat in a rigid, stationary chair to reduce movement artifacts.

262 After fitting the fNIRS cap to the participant's head, signal quality was checked for each source-
263 detector channel and calibrated if needed to make sure the fNIRS fiber optics made good contact with the
264 scalp of the participant, and that the detector was sensitive to cardiac pulsation as a sign of good signal-
265 to-noise (SNR) ratio. Any detector saturation was also adjusted for in this step. fNIRS data was recorded
266 for each participant using custom data collection software that interfaced with the fNIRS system, described
267 in [43].

268

269

270 -----

271 **Fig. 2. Probe layout for Experiment 1.** Sources are in red and detectors are in blue. Channels are in
272 black, labeled 1-5 on the right hemisphere and 6-10 on the left.

273 -----

274

275 **fNIRS Data Processing**

276

277 Raw light attenuation measurements were converted to oxy-hemoglobin and deoxy-hemoglobin
278 concentration changes using the modified Beer-Lambert law [44,45]. We removed long-term drifts in the
279 data by subtracting a least-squares linear fit. We then band-pass filtered the data to remove cardiac and
280 respiration signals (retaining frequencies in the range 0.01-0.1 Hz, as suggested by [40]). To mitigate
281 motion artifacts in the form of sudden spikes or shifts, we applied a widely-used correlation based signal
282 improvement (CBSI) filter, which is based on the assumption that true oxy-Hb and deoxy-Hb should be
283 maximally negatively correlated [46]. As an alternative, we also ran all of the analyses on data filtered
284 with a kurtosis-based wavelet filter (kbWF), shown previously to outperform other motion artifact

285 removal methods such as PCA, tPCA, regular wavelet filter, and spline interpolation [47] -- results with
286 the kbWF were qualitatively identical and hence not reported here. With the resulting time series, we
287 computed partial correlations for each channel pair (CP), given the other channels (since there were 10
288 channels, there were 45 (10 choose 2) distinct CPs). These 45 computed partial correlations, which are
289 represented graphically in correlation matrices (as in Figure 3) were the main quantities studied in this
290 paper. We used partial correlation as the index of RSFC in this study because it can factor out correlation
291 between fNIRS channels due to shared extracerebral components, and is thus thought to characterize
292 relationships between brain regions more precisely than Pearson's correlation [48,49].

293

294 **Data Analysis Strategy**

295

296 Our first goal was to test for significant homologous connectivity, characteristic of RSFC. To do
297 this, we compared functional connectivity between regions that were homologous (bilaterally symmetric)
298 to that between non-homologous regions.

299 Our second goal was to test the validity of Freeplay as a task for measuring resting state. To do so, we
300 compared the functional connectivity in adults between the two conditions, "at rest" and Freeplay. Since
301 it is difficult to directly measure similarity between two groups of functional connectivity patterns, we did
302 so by estimating the accuracy of classifiers trained to distinguish different conditions (e.g., between "at
303 rest" and Freeplay in adults). Higher accuracies suggest greater distinguishability, and hence greater
304 dissimilarity, between classes. Given the high-dimensionality (45 CPs) of our problem, we used logistic
305 LASSO (i.e., logistic regression with the Least Absolute Selection and Shrinkage Operator penalty), which
306 should perform relatively well in our high-dimensional setting [50]. Accuracy was estimated using leave-
307 one-out cross-validation (LOOCV). Within each LOOCV fold, the LASSO regularization parameter λ
308 was selected by 10-fold cross validation. To reduce the chance that results were classifier specific, we also

309 tried a highly distinct classifier, k-nearest neighbors (kNN) classification. Accuracy was again estimated
310 by LOOCV, with k selected within each LOOCV fold by 10-fold cross-validation (over $k=1, \dots, 10$,
311 covering a range of common values [51]). To provide a baseline for comparison, we similarly compared
312 data from adults versus children in Freeplay.

313

314 **Results**

315

316 First and foremost, all participants (including all child participants) completed the task and
317 provided usable data.

318

319

320

321 **Fig. 3. Group-averaged partial correlation matrices for children in Freeplay and for adults in**
322 **Freeplay and at rest.** Channels 1-5 were located on the right hemisphere; channels 6-10 were located on
323 the left hemisphere. Homologous CPs are circled in the child panel.

324

325

326 **Homologous versus non-homologous CPs**

327

328 First, we compared all homologous to all non-homologous pairs of distinct channels, to identify
329 the strong inter-hemispheric homologous connections. Specifically, we averaged homologous and non-
330 homologous CPs within subjects, forming two sets of measured CP correlations (r -values; separately for
331 adults and children). This comparison showed that homologous CPs were significantly more strongly

332 connected than non-homologous CPs ($p < 0.001$ for both children and adults, by a two-sample t -test of the
333 Fisher z -transformed r -values as well as a permutation test).

334

335

336 **Adult correlations in Freeplay versus “at rest”**

337

338 Next, we compared adult correlations in Freeplay and “at rest” to see how Freeplay compares with
339 traditional resting state. Logistic LASSO, trained to predict Freeplay or “at rest” from CP correlations,
340 gave a LOOCV accuracy of 38.462% (worse than chance, 50%), suggesting that the two tasks do not seem
341 to elicit highly distinct connectivity (95% Wilson score confidence interval (CI): [19.76%, 57.16%]). The
342 kNN classification to predict Freeplay or “at rest” from CP correlations achieved a LOOCV classification
343 accuracy of 57.7% (95% Wilson score confidence interval (CI): [48.32%, 67.08%]), just over chance.

344

345 **Adult versus child correlations in Freeplay**

346

347 Next, we compared correlation matrices between adults and children, both in Freeplay. Logistic
348 LASSO, trained to predict “adult” or “child” from CP correlations, gave a LOOCV accuracy of 83.333%,
349 suggesting that adults and children exhibit highly distinct connectivity in Freeplay (95% Wilson score
350 confidence interval (CI): [69.997%, 96.669%]).

351

352 **Experiment 2: Test-retest reliability with children in Freeplay**

353

354 In this experiment, we studied reliability of the NIRS- Freeplay RSFC measure in children, in
355 terms of consistency of results across independent scans (intersession, or test-retest, reliability). To do

356 this, we collected multiple NIRS-Freeplay scans from children on different days and estimate a
357 connectivity network from each scan. We then measured similarity of this estimated connectivity network
358 both across scans within subjects and across subjects.

359

360 **Methods**

361 **Participants**

362

363 Participants consisted of 19 children (aged 3 to 5 years, M_{age} during first scan = 4.34, M_{age} during
364 second scan = 4.65, Med_{age} during first scan = 4.31, M_{age} during second scan = 4.82) recruited from the
365 Children's School. Data was collected longitudinally at 2 time points (on average 3.7 months apart), with
366 2 scans (approximately 1 week apart) at each time point. These data were collected as part of a bigger
367 study, and the longitudinal aspect was not analyzed in this study. 17 participants completed all 4 scans;
368 data from 2 participants who were not able to complete all 4 scans due to scheduling constraints was
369 discarded.

370

371

372

373 **Fig. 4. Probe layout for Experiment 2.** Sources are in red and detectors are in blue. Channels are in
374 black, labeled 1-5 on the right hemisphere and 6-10 on the left.

375

376

377 **Freeplay and fNIRS Set-up**

378

379 The Freeplay set-up was as in Experiment 1. fNIRS set-up was almost identical to that in

380 Experiment 1, with 4 light sources and 8 detectors, to give oxygenation measures in 10 channels on the
381 prefrontal cortex, except with a slightly different sensor layout as depicted in Figure 4.

382

383 **fNIRS Data Processing**

384

385 Data was preprocessed and partial correlations computed as in Experiment 1. Again, since there
386 were 10 channels in this probe design, there were 45 (10 choose 2) distinct CPs.

387

388 **Measures of within vs. between subject variance**

389

390 Kendall's W and intra-class correlation (ICC) are measures of concordance between groups,
391 frequently used to study test-retest reliability in fMRI data [52-54,17]. In particular, these measures
392 quantify the degree to which scans from the same participant agree compared to scans between different
393 participants. Kendall's W and ICC both range from 0 to 1, where values approaching 1 indicate high
394 stability of inter-participant variability -- that is, scans are highly reproducible and unique within
395 participants. Smaller values (approaching 0) indicate low stability of inter-participant variability, where
396 scans are highly variable within participants and not differentiable between participants.

397 Kendall's W and ICC are defined for a given CP as follows. Given ranks (over subjects) of the
398 RSFC in that CP (in each scan), Kendall's W is the mean (over subjects) of the squared deviation of the
399 sum (over scans) of the ranks. That is, if m is the number of scans and n is the number of subjects, if r_{ij}
400 denotes the rank of the i^{th} subject's RSFC in scan j , then Kendall's W is defined by the following set of
401 equations:

$$402 \quad R_i = \sum_{j=1}^m r_{ij}, \quad \bar{R} = \frac{1}{n} \sum_{i=1}^n R_i \quad (1)$$

403
$$S = \sum_{i=1}^n (R_i - \bar{R})^2, \quad W = \frac{12S}{m^2(n^3 - n)}. \quad (2)$$

404 ICC is defined as the proportion of between subjects variation to total variation. That is,

405
$$ICC = \frac{BSV}{BSV + WSV}$$

406 where BSV denotes the between-subjects variance (i.e., the average (over scans) of the variance across
407 subjects) and WSV denotes the within-subjects variance (i.e., the average (over subjects) of the variance
408 across scans).

409

410 **Measures of similarity between binarized connectivity networks**

411

412 In addition to the partial correlation matrix itself, studies of RSFC are often interested in the
413 network structure of functional connectivity. Studying this requires binarizing the partial correlation
414 matrix (i.e., identifying each CP as either “connected” or “disconnected”. Therefore, to study reliability
415 of the functional connectivity network, we binarized each CP by thresholding the absolute value of its
416 partial correlation value at a “connectivity threshold” θ ; absolute values below θ were replaced with 0
417 (denoting an unconnected CP), and absolute values above θ replaced by 1 (denoting a connected CP).

418 We then used two indices of inter-scan reliability: the F1 score (a.k.a., Dice coefficient), a general
419 measure of overlap between two sets (twice the ratio of the number of CPs functionally connected in *both*
420 scans to the sum of the numbers of functionally connected CPs over both scans) and the Matthews
421 correlation coefficient (MCC), the correlation between the binarized pattern of 0’s and 1’s, across all 45
422 CPs. Accuracy (proportion of agreement) between the two binarized scans was not used as a measure of
423 similarity because it is extremely sensitive to the connectivity threshold; for example, using a threshold
424 of 0 (full connectivity) or 1 (no connectivity) results in a perfect accuracy of 1. The raw (continuous, un-

425 thresholded) correlation was also not used, as it is relatively difficult to interpret as a measure of reliability.
426 We chose θ to maximize (over 1000 equally spaced values between 0 and 1) each reliability index (F1
427 score and MCC) and used LOOCV to obtain an unbiased estimate of each reliability index.

428

429

430 **Results**

431

432 **Group-level RSFC correlation**

433

434 The calculated Pearson and Spearman correlations between mean (across subject) RSFC matrices
435 in each scan (lower triangle of the matrices, excluding main diagonal) were 0.95 with 95% Confidence
436 Interval (CI) (0.88, 0.96) (deoxy-Hb: 0.95 with 95% CI (0.89, 0.95)) and 0.85 with 95% CI (0.64,0.90)
437 (deoxy-Hb: 0.85 with 95% CI (0.58, 0.90)), respectively. This scan1-scan2 correlation for each channel
438 pair is plotted in Figure 5 (panel (c)), along with visualizations of the group level RSFC matrices (panels
439 (a) and (b)). The strong correlation values suggest that conclusions drawn from RSFC group-level matrices
440 should be fairly reproducible. Figure 5(c) also suggests that the presence of adjacent channel pairs, which
441 tend to be strongly functionally connected, skews the RSFC distributions to the right. However, stronger
442 correlations of homologous pairs compared to the rest (non-homologous or adjacent) are still observed.
443 Nevertheless, we investigated the effects of adjacent channel pairs by also running all the analyses with
444 adjacent channels removed – the results are discussed in the section “Post-hoc tests” below.

445 To also measure consistency across scans at the individual level, we calculated Pearson and
446 Spearman correlations between RSFC matrices in each scan, for each subject. The average of those
447 correlations was 0.47 with 95% CI (0.42,0.53) (deoxy-Hb: 0.47 with 95% CI (0.42, 0.54)) for Pearson and

448 0.43 with 95% CI (0.37, 0.49) (deoxy-Hb: 0.42 with 95% (0.36, 0.48)) for Spearman, suggesting that
449 consistent, detectable signals are present even at the individual level.

450

451

452 -----

453 **Fig. 5. Correlation matrices for scans 1 and 2.** Plot of correlation between the two correlation maps
454 shown on the right. Each point corresponds to a CP. Adjacent and homologous CPs, which consistently
455 exhibit stronger functional connectivities, are distinguished from other CPs.

456 -----

457

458 **Within vs. between subject variance**

459

460 Kendall's W values (across subjects, between scans, for each CP) had a significantly positive mean
461 (across CPs) of 0.55, with 95% CI (0.52, 0.60) (deoxy-Hb: 0.55 with 95% CI (0.50, 0.59)). Similarly, ICC
462 values (across subjects, between scans), also calculated for each CP, were significantly positive, with a
463 mean of 0.53 with 95% CI (0.51, 0.55) (deoxy-Hb: 0.52 with 95% CI (0.50, 0.55)). Both of these results
464 reflect greater consistency within subjects (or smaller within-subject variance) than between subjects.

465

466 **Consistency of connectivity patterns**

467

468 The mean (across LOOCV folds) F1 score was 0.71 with 95% CI (0.66, 0.76) (deoxy-Hb: 0.67
469 with 95% CI (0.63, 0.71)). The mean cutoff threshold chosen was $\theta=0.73$, corresponding to functional
470 connectivity in a mean of 6.4% of CPs. The mean MCC was 0.44 with 95% CI (0.37, 0.51) (deoxy-Hb:
471 0.39 with 95% CI (0.29,0.49)), with a mean cutoff threshold of $\theta=0.66$, corresponding to functional

472 connectivity in a mean of 9.4% of CPs. Within each cross-validation fold, a nested LOOCV was used to
473 select the thresholds that maximized the reliability score. The entire cross-validation curves are shown in
474 Figure 6.

475 We performed a permutation test comparing the F1 score or MCC to that after randomly permuting
476 the CPs in the second scan for each participant, to test a null model where CPs are randomly identified as
477 functionally connected, with the two scans independent. This test rejected the null for both F1 score and
478 MCC ($p < 0.01$; 1000 permutations). That is, within subjects, we find functional connectivity consistently
479 in the same channels between scans.

480 Interestingly, similar tests in which second scans were randomly permuted across *participants* (i.e., for
481 a null model of identical/non-distinct participants) were *not* significant ($p > 0.05$), suggesting consistency
482 *across* subjects in Freeplay. This is encouraging from the perspective of trying to identify a common
483 pattern of functional connectivity across individuals. However, further work is needed to understand the
484 sensitivity of the paradigm to individual differences (that may correlate with other quantities of interest,
485 such as age, or behavioral measures), for which we conjecture that the continuous (un-thresholded) CP
486 correlations may be more informative.

487

488

489 **Fig. 6. Plot of reliability for each measure over threshold values ranging from 0 to 1.** Thin lines show
490 bootstrapped 95% confidence bands. The threshold that maximizes reliability was the same for both F1
491 and MCC, as indicated by the vertical orange line. For F1 and MCC, reliability is undefined when the
492 entries are all 0 or all 1.

493

494

495 **Post-hoc tests**

496

497 As is apparent from the group RSFC matrices shown in Figures 2 and 4, adjacent channels are
498 quite strongly correlated with each other -- thus, it is possible that the consistent patterns we detected were
499 driven primarily by these correlations between adjacent channels. To test for this possibility, we re-ran all
500 of the concordance tests after removing adjacent channel pair correlations from the RSFC matrix. The
501 results are shown in Table 1. Although significance levels were generally reduced, all tests that had been
502 significant when adjacent channels were included continued to be significant after their removal, at alpha
503 level 0.05.

504

505 **Tab. 1. Results excluding adjacent channels.**

Quantity	Oxy (95% CI)	Deoxy (95% CI)
Pearson (Group)	0.75 (0.32, 0.77)	0.74 (0.46, 0.78)
Spearman (Group)	0.71 (0.43, 0.75)	0.71 (0.34, 0.78)
Pearson (Subject)	0.18 (0.09, 0.26)	0.18 (0.09, 0.25)
Spearman (Subject)	0.17 (0.06, 0.25)	0.17 (0.07, 0.25)
Kendall's W	0.55 (0.50, 0.61)	0.55 (0.49, 0.59)
ICC	0.53 (0.49, 0.55)	0.53 (0.50, 0.56)
F1	0.51 (0.47, 0.54)	0.52 (0.49, 0.54)
MCC	0.05 (-0.01, 0.12)	0.06 (0.00, 0.13)

506

507

508 **Summary of results**

509

510 This study explored the feasibility of using fNIRS and Freeplay to measure RSFC in children.
511 Consistent with previous results, we were able to recover connectivity features characteristic of RSFC,
512 helping validate our fNIRS set-up for measuring traditional RSFC. More specifically, homologous
513 channel pairs were significantly more correlated than non-homologous channel pairs, consistent with
514 previous results which found higher coherence between bilateral homologous region pairs than in fronto-
515 posterior pairs or arbitrary pairs in adults [40,41].

516 Additionally, in adults, correlation patterns in Freeplay were similar to that in traditional resting
517 state -- trained classifiers did not perform significantly better than chance, suggesting that Freeplay may
518 produce a state similar to that in the traditional resting state condition. Since Freeplay was designed to
519 approximate resting state in children, who struggle with the traditional resting state task, this comparison
520 of Freeplay to the traditional task in adult participants serves as an additional check for the viability of
521 fNIRS-Freeplay for measuring RSFC in children. Crucially, all children completed the task and provided
522 usable data, speaking to the practical utility of the Freeplay paradigm for studying RSFC in children.
523 Further, correlations in adults and children in Freeplay showed different patterns, from which a trained
524 classifier was able to predict “adult” or “child” with high accuracy -- this is in line with our expectations
525 given that we know RSNs develop significantly with age. Finally, Experiment 2 demonstrated inter-scan
526 reliability, in that similar connectivity patterns are found between 2 independent scans of the same
527 individual, and that within-subject variance is significantly lower than between-subject variance. This
528 reliability is observed for both the raw RSFC matrices and the resulting connectivity networks after
529 thresholding appropriately, and is observed both with and without adjacent channel pairs.

530

531 **Limitations and future directions**

532

533 The test-retest reliability value for ICC (0.53) was lower in our paper than in a previous paper (0.7)
534 by Niu et al. looking at RSFC test-retest reliability in adults [19]. Some possible reasons for this may be
535 that: 1) since we are measuring in children, the data may be noisier, and 2) they measured functional
536 connectivity in terms of Pearson (rather than partial) correlations, which can be inflated by other sources
537 of correlation between channels besides functional brain correlations.

538 Although our study compared “Freeplay” to the traditional “at rest” condition measured with adults,
539 it did not compare to either a true task condition, or a “movie-watching” condition. Comparing the
540 functional connectivity patterns in “Freeplay” with not just “at rest” but also these other conditions may
541 help us better characterize RSFC. For example, if we are able to show that a trained classifier can
542 effectively distinguish between adults in the “at rest” or “Freeplay” conditions from those in the movie
543 watching condition, it would provide a comparison condition for “Freeplay” as well as corroborate
544 previous findings that “movie watching” alters resting state.

545 The current study introduced a new paradigm for measuring resting state functional connectivity
546 in children that combines fNIRS and a method called Freeplay to help increase participant compliance
547 and induce a state similar to adult resting state in children. We demonstrated the practical feasibility as
548 well as the construct validity of the Freeplay-fNIRS paradigm for studying RSFC in children by measuring
549 correlations between pairs of regions in the PFC. As previously discussed, the PFC is a central player in
550 the central executive network (CEN), and studying its RSFC patterns over development is crucial to
551 understanding how the CEN develops and supports executive function (EF). Zhao et al. [55] recently
552 found that network properties of RSFC in the PFC, as measured by fNIRS, were correlated with varying
553 performance in EF tasks in adults. An important next step will be to extend those investigations to children.
554 Future work can explore the changes in PFC connectivity structures that parallel observed cognitive

555 development in EF or other domains subserved by the PFC. As a practical setup for measuring RSFC in
556 children, the fNIRS-Freeplay paradigm will allow investigation of questions such as these to advance
557 understanding of the neural mechanisms of cognitive development.

558

559 **Acknowledgements**

560

561 We thank the children, parents, and teachers of the CMU Children's School for making this work possible.

562

563

564

565 **References**

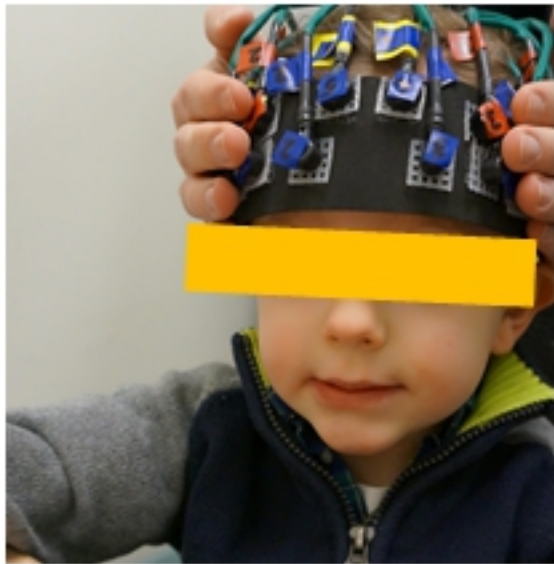
566

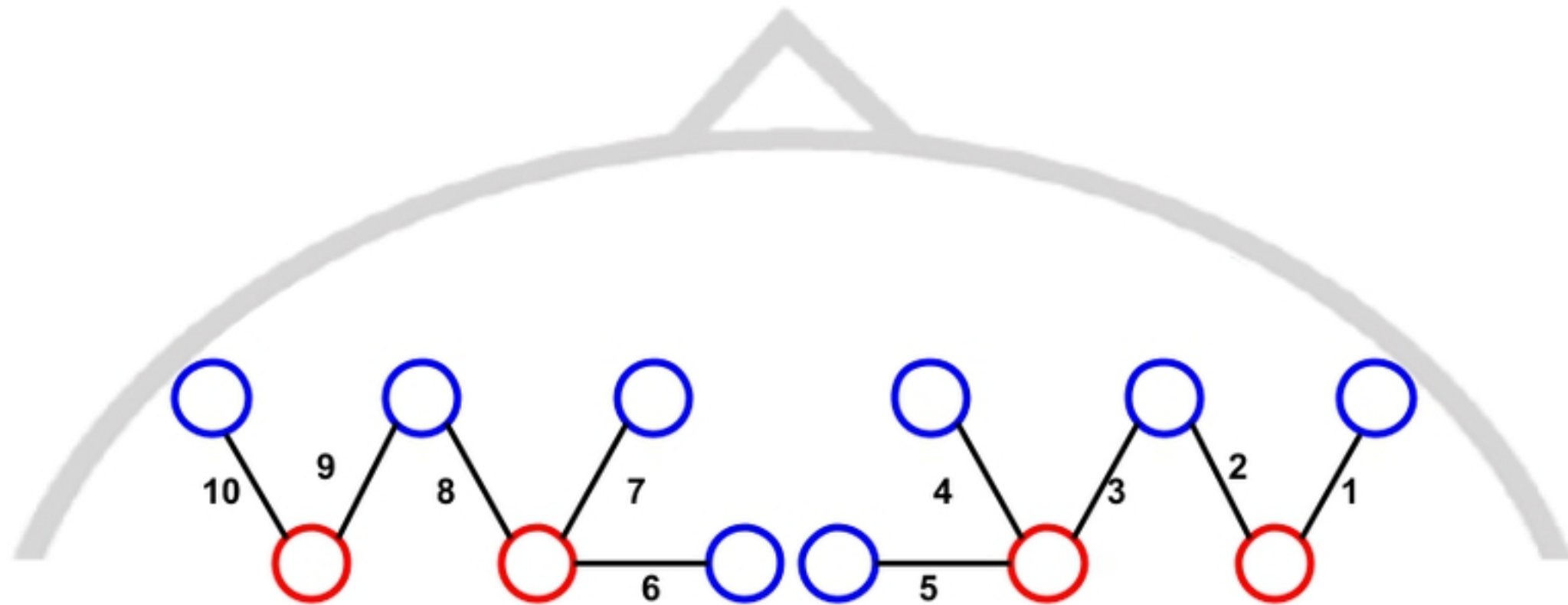
- 567 [1] Moussa MN, Steen MR, Laurienti PJ, Hayasaka S. Consistency of network modules in resting-state
568 fMRI connectome data. *PloS one*. 2012 Aug 31;7(8):e44428.
- 569 [2] Friston KJ. Functional and effective connectivity in neuroimaging: a synthesis. *Human brain mapping*.
570 1994;2(1-2):56-78.
- 571 [3] Rosazza, C., & Minati, L. (2011). Resting-state brain networks: literature review and clinical
572 applications. *Neurological Sciences*, 32(5), 773-785.
- 573 [4] Fox MD, Raichle ME. Spontaneous fluctuations in brain activity observed with functional magnetic
574 resonance imaging. *Nature reviews neuroscience*. 2007 Sep;8(9):700.
- 575 [5] Biswal, B., Zerrin Yetkin, F., Haughton, V. M., & Hyde, J. S. (1995). Functional connectivity in the
576 motor cortex of resting human brain using echo-planar mri. *Magnetic resonance in medicine*, 34(4), 537-
577 541.
- 578 [6] Cordes, D., Haughton, V. M., Arfanakis, K., Wendt, G. J., Turski, P. A., Moritz, C. H., ... & Meyerand,
579 M. E. (2000). Mapping functionally related regions of brain with functional connectivity MR imaging.
580 *American Journal of Neuroradiology*, 21(9), 1636-1644.
- 581 [7] Seeley, W. W., Menon, V., Schatzberg, A. F., Keller, J., Glover, G. H., Kenna, H., ... & Greicius, M.
582 D. (2007). Dissociable intrinsic connectivity networks for salience processing and executive control.
583 *Journal of Neuroscience*, 27(9), 2349-2356.
- 584 [8] Stevens, W. D., Buckner, R. L., & Schacter, D. L. (2009). Correlated low-frequency BOLD
585 fluctuations in the resting human brain are modulated by recent experience in category-preferential visual
586 regions. *Cerebral cortex*, 20(8), 1997-2006.
- 587 [9] Jolles DD, van Buchem MA, Crone EA, Rombouts SA. A comprehensive study of whole-brain
588 functional connectivity in children and young adults. *Cerebral cortex*. 2010 Jun 11;21(2):385-91.
- 589 [10] Barkhof F, Haller S, Rombouts SA. Resting-state functional MR imaging: a new window to the
590 brain. *Radiology*. 2014 Jul;272(1):29-49.
- 591 [11] Supekar K, Musen M, Menon V. Development of large-scale functional brain networks in children.
592 *PLoS biology*. 2009 Jul 21;7(7):e1000157.
- 593 [12] Fair DA, Cohen AL, Power JD, Dosenbach NU, Church JA, Miezin FM, Schlaggar BL, Petersen
594 SE. Functional brain networks develop from a “local to distributed” organization. *PLoS computational*
595 *biology*. 2009 May 1;5(5):e1000381.

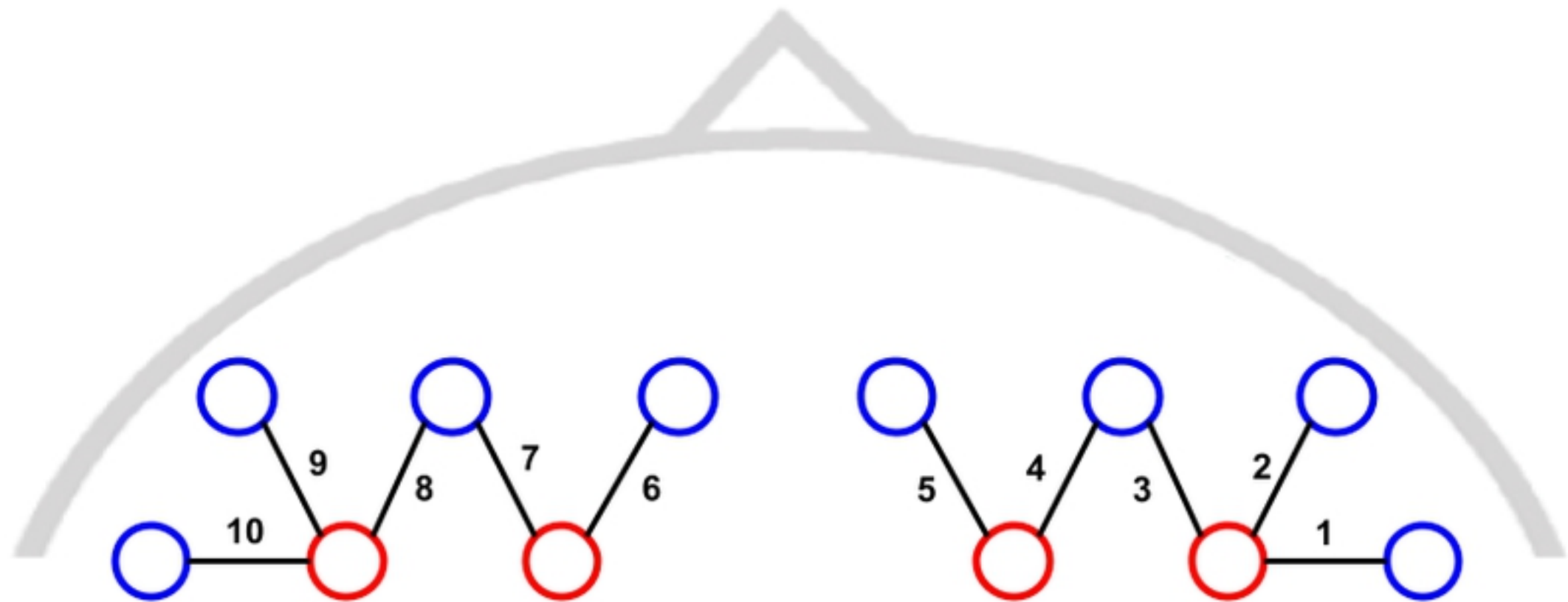
- 596 [13] Byars AW, Holland SK, Strawsburg RH, Bommer W, Dunn RS, et al. (2002): Practical aspects of
597 conducting large-scale functional magnetic resonance imaging studies in children. *J Child Neurol*
598 17:885–889.
- 599 [14] Yerys BE, Jankowski KF, Shook D, Rosenberger LR, Barnes KA, Berl MM, Ritzl EK, VanMeter J,
600 Vaidya CJ, Gaillard WD. The fMRI success rate of children and adolescents: typical development,
601 epilepsy, attention deficit/hyperactivity disorder, and autism spectrum disorders. *Human brain mapping*.
602 2009 Oct;30(10):3426-35.
- 603 [15] Betti V, Della Penna S, de Pasquale F, Mantini D, Marzetti L, Romani GL, Corbetta M. Natural
604 scenes viewing alters the dynamics of functional connectivity in the human brain. *Neuron*. 2013 Aug
605 21;79(4):782-97.
- 606 [16] Uddin LQ, Supekar K, Menon V. Typical and atypical development of functional human brain
607 networks: insights from resting-state FMRI. *Frontiers in systems neuroscience*. 2010 May 21;4:21.
- 608 [17] Thomason ME, Dennis EL, Joshi AA, Joshi SH, Dinov ID, Chang C, Henry ML, Johnson RF,
609 Thompson PM, Toga AW, Glover GH. Resting-state fMRI can reliably map neural networks in children.
610 *Neuroimage*. 2011 Mar 1;55(1):165-75.
- 611 [18] Braun U, Plichta MM, Esslinger C, Sauer C, Haddad L, Grimm O, Mier D, Mohnke S, Heinz A, Erk
612 S, Walter H. Test–retest reliability of resting-state connectivity network characteristics using fMRI and
613 graph theoretical measures. *Neuroimage*. 2012 Jan 16;59(2):1404-12.
- 614 [19] Niu H, Li Z, Liao X, Wang J, Zhao T, Shu N, Zhao X, He Y. Test-retest reliability of graph metrics
615 in functional brain networks: a resting-state fNIRS study. *PLoS One*. 2013 Sep 9;8(9):e72425.
- 616 [20] Geng S, Liu X, Biswal BB, Niu H. Effect of resting-state fNIRS scanning duration on functional
617 brain connectivity and graph theory metrics of brain network. *Frontiers in neuroscience*. 2017 Jul
618 20;11:392.
- 619 [21] Raschle N, Zuk J, Ortiz-Mantilla S, Sliva DD, Franceschi A, Grant PE, Benasich AA, Gaab N.
620 Pediatric neuroimaging in early childhood and infancy: challenges and practical guidelines. *Annals of*
621 *the New York Academy of Sciences*. 2012 Apr;1252:43.
- 622 [22] Power JD, Barnes KA, Snyder AZ, Schlaggar BL, Petersen SE. Spurious but systematic correlations
623 in functional connectivity MRI networks arise from subject motion. *Neuroimage*. 2012 Feb 1;59(3):2142-
624 54.
- 625 [23] Nishiyori R. fNIRS: An emergent method to document functional cortical activity during infant
626 movements. *Frontiers in psychology*. 2016 Apr 20;7:533.
- 627 [24] Patriat R, Molloy EK, Meier TB, Kirk GR, Nair VA, Meyerand ME, Prabhakaran V, Birn RM. The
628 effect of resting condition on resting-state fMRI reliability and consistency: a comparison between resting
629 with eyes open, closed, and fixated. *Neuroimage*. 2013 Sep 1;78:463-73.
- 630 [25] Liu WC, Flax JF, Guise KG, Sukul V, Benasich AA. Functional connectivity of the sensorimotor
631 area in naturally sleeping infants. *Brain research*. 2008 Aug 5;1223:42-9.
- 632 [26] Horovitz SG, Fukunaga M, de Zwart JA, van Gelderen P, Fulton SC, Balkin TJ, Duyn JH. Low
633 frequency BOLD fluctuations during resting wakefulness and light sleep: A simultaneous EEG-fMRI
634 study. *Human brain mapping*. 2008 Jun;29(6):671-82.
- 635 [27] Horovitz SG, Braun AR, Carr WS, Picchioni D, Balkin TJ, Fukunaga M, Duyn JH. Decoupling of
636 the brain's default mode network during deep sleep. *Proceedings of the National Academy of Sciences*.
637 2009 Jul 7;106(27):11376-81.
- 638 [28] Boly M, Perlberg V, Marrelec G, Schabus M, Laureys S, Doyon J, Péligrini-Issac M, Maquet P,
639 Benali H. Hierarchical clustering of brain activity during human nonrapid eye movement sleep.
640 *Proceedings of the National Academy of Sciences*. 2012 Apr 10;109(15):5856-61.
- 641 [29] Spoomaker VI, Gleiser P, Czisch M. Frontoparietal connectivity and hierarchical structure of the
642 brain's functional network during sleep. *Frontiers in neurology*. 2012 May 17;3:80.

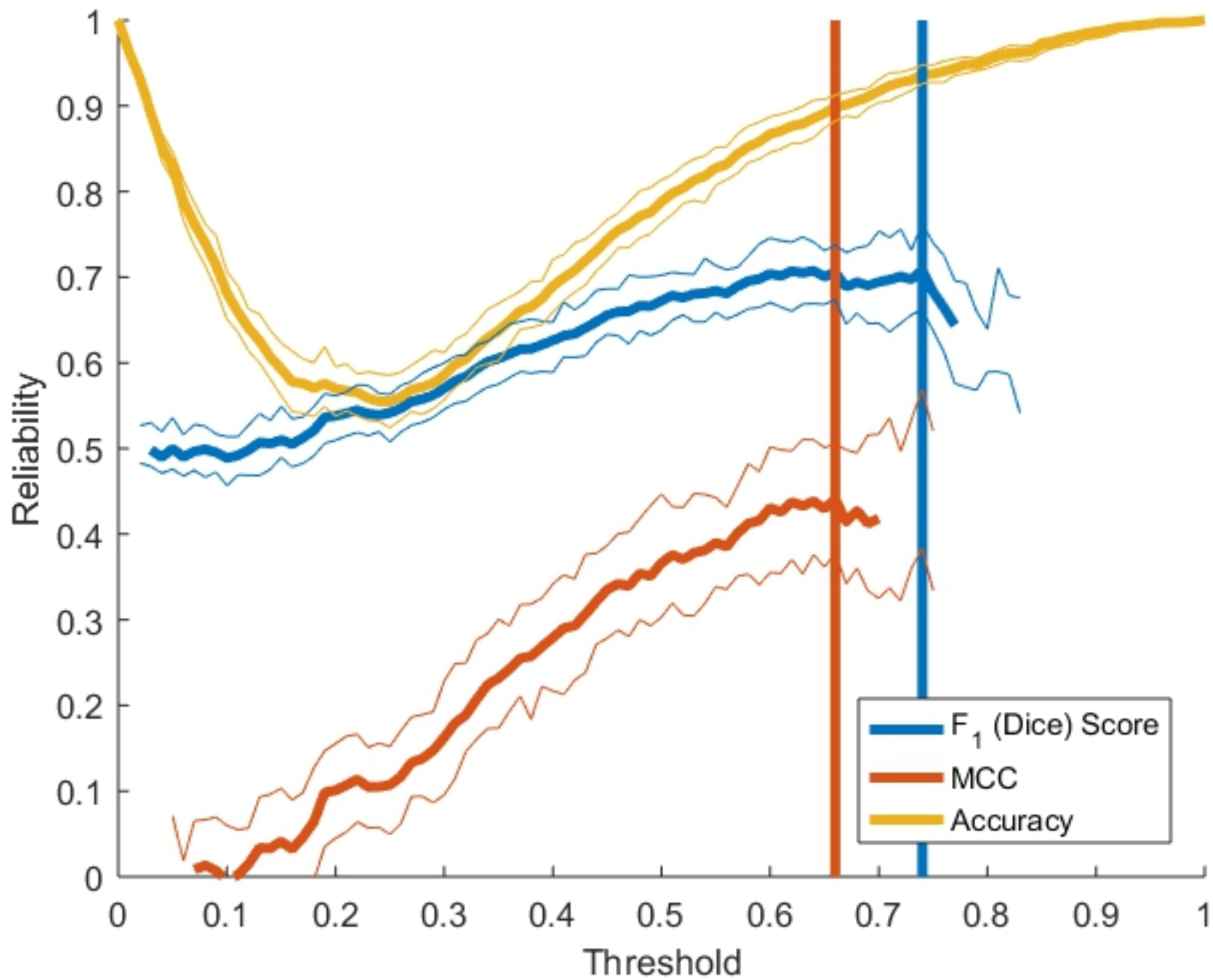
- 643 [30] de Bie HM, Boersma M, Wattjes MP, Adriaanse S, Vermeulen RJ, Oostrom KJ, Huisman J, Veltman
644 DJ, Delemarre-Van de Waal HA. Preparing children with a mock scanner training protocol results in
645 high quality structural and functional MRI scans. *European journal of pediatrics*. 2010 Sep
646 1;169(9):1079-85.
- 647 [31] Greene DJ, Koller JM, Hampton JM, Wesevich V, Van AN, Nguyen AL, Hoyt CR, McIntyre L,
648 Earl EA, Klein RL, Shimony JS. Behavioral interventions for reducing head motion during MRI scans
649 in children. *NeuroImage*. 2018 May 1;171:234-45.
- 650 [32] Barker JW, Aarabi A, Huppert TJ. Autoregressive model based algorithm for correcting motion and
651 serially correlated errors in fNIRS. *Biomedical optics express*. 2013 Aug 1;4(8):1366-79.
- 652 [33] Emerson RW, Short SJ, Lin W, Gilmore JH, Gao W. Network-level connectivity dynamics of movie
653 watching in 6-year-old children. *Frontiers in human neuroscience*. 2015 Nov 23;9:631.
- 654 [34] Cantlon JF, Li R. Neural activity during natural viewing of Sesame Street statistically predicts test
655 scores in early childhood. *PLoS biology*. 2013 Jan 3;11(1):e1001462.
- 656 [35] Vanderwal T, Kelly C, Eilbott J, Mayes LC, Castellanos FX. Inscapes: A movie paradigm to improve
657 compliance in functional magnetic resonance imaging. *Neuroimage*. 2015 Nov 15;122:222-32.
- 658 [36] Casey BJ, Giedd JN, Thomas KM. Structural and functional brain development and its relation to
659 cognitive development. *Biological psychology*. 2000 Oct 1;54(1-3):241-57.
- 660 [37] Diamond A. The early development of executive functions. *Lifespan cognition: Mechanisms of*
661 *change*. 2006;210:70-95.
- 662 [38] Diamond A. Executive functions. *Annual review of psychology*. 2013 Jan 3;64:135-68.
- 663 [39] Lin HY, Tseng WY, Lai MC, Matsuo K, Gau SS. Altered resting-state frontoparietal control network
664 in children with attention-deficit/hyperactivity disorder. *Journal of the International Neuropsychological*
665 *Society*. 2015 Apr;21(4):271-84.
- 666 [40] Sasai S, Homae F, Watanabe H, Taga G. Frequency-specific functional connectivity in the brain
667 during resting state revealed by NIRS. *Neuroimage*. 2011 May 1;56(1):252-7.
- 668 [41] Sasai S, Homae F, Watanabe H, Sasaki AT, Tanabe HC, Sadato N, Taga G. A NIRS-fMRI study of
669 resting state network. *Neuroimage*. 2012 Oct 15;63(1):179-93.
- 670 [42] Wang J, Dong Q, Niu H. The minimum resting-state fNIRS imaging duration for accurate and stable
671 mapping of brain connectivity network in children. *Scientific reports*. 2017 Jul 25;7(1):6461.
- 672 [43] Abdelnour AF, Huppert T. Real-time imaging of human brain function by near-infrared
673 spectroscopy using an adaptive general linear model. *Neuroimage*. 2009 May 15;46(1):133-43.
- 674 [44] Huppert TJ. History of diffuse optical spectroscopy of human tissue. In *Optical Methods and*
675 *Instrumentation in Brain Imaging and Therapy 2013* (pp. 23-56). Springer, New York, NY.
- 676 [45] Whiteman AC, Santosa H, Chen DF, Perlman SB, Huppert T. Investigation of the sensitivity of
677 functional near-infrared spectroscopy brain imaging to anatomical variations in 5-to 11-year-old children.
678 *Neurophotonics*. 2017 Sep;5(1):011009.
- 679 [46] Cui X, Bray S, Reiss AL. Functional near infrared spectroscopy (NIRS) signal improvement based
680 on negative correlation between oxygenated and deoxygenated hemoglobin dynamics. *Neuroimage*. 2010
681 Feb 15;49(4):3039-46.
- 682 [47] Chiarelli AM, Maclin EL, Fabiani M, Gratton G. A kurtosis-based wavelet algorithm for motion
683 artifact correction of fNIRS data. *Neuroimage*. 2015 May 15;112:128-37.
- 684 [48] Sakakibara E, Homae F, Kawasaki S, Nishimura Y, Takizawa R, Koike S, Kinoshita A, Sakurada
685 H, Yamagishi M, Nishimura F, Yoshikawa A. Detection of resting state functional connectivity using
686 partial correlation analysis: A study using multi-distance and whole-head probe near-infrared
687 spectroscopy. *NeuroImage*. 2016 Nov 15;142:590-601.
- 688 [49] Marrelec G, Krainik A, Duffau H, Pélégriani-Issac M, Lehericy S, Doyon J, Benali H. Partial
689 correlation for functional brain interactivity investigation in functional MRI. *Neuroimage*. 2006 Aug
690 1;32(1):228-37.

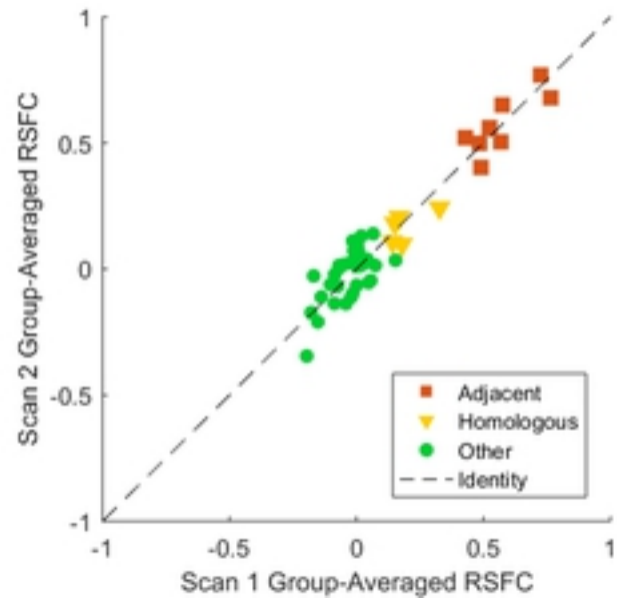
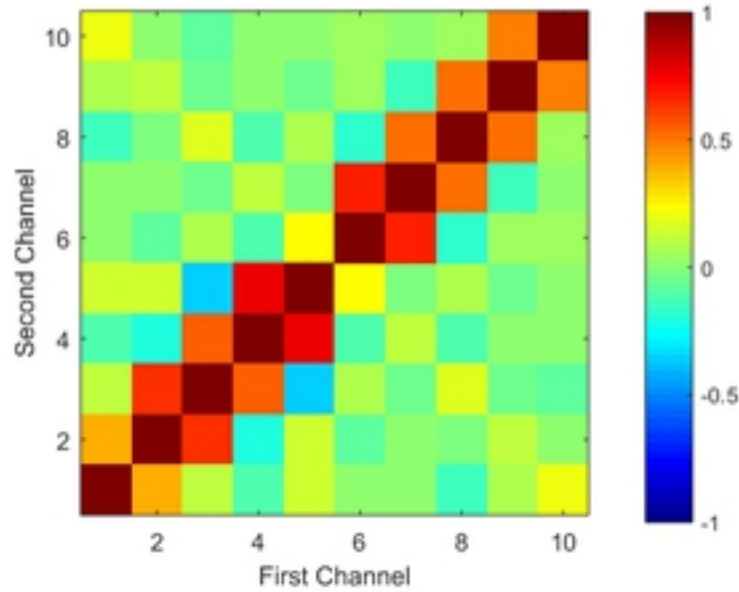
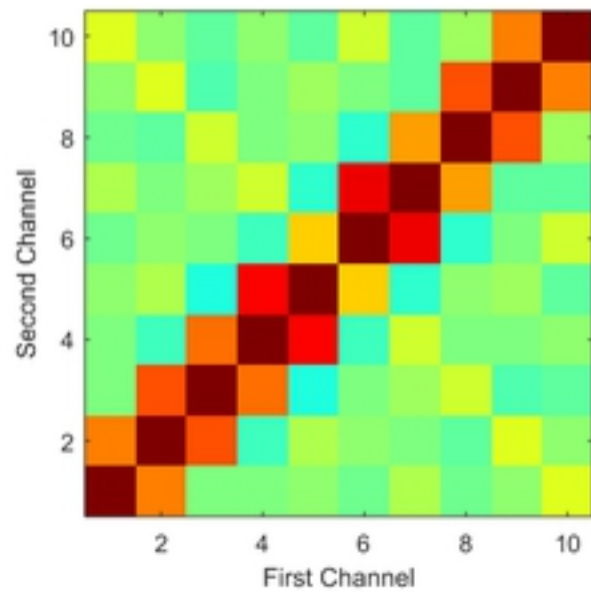
- 691 [50] Tibshirani R. Regression shrinkage and selection via the lasso. *Journal of the Royal Statistical*
692 *Society: Series B (Methodological)*. 1996 Jan;58(1):267-88.
- 693 [51] Cunningham P, Delany SJ. k-Nearest neighbour classifiers. *Multiple Classifier Systems*. 2007 Mar
694 27;34(8):1-7.
- 695 [52] Caceres A, Hall DL, Zelaya FO, Williams SC, Mehta MA. Measuring fMRI reliability with the intra-
696 class correlation coefficient. *Neuroimage*. 2009 Apr 15;45(3):758-68.
- 697 [53] Meltzer JA, Postman-Caucheteux WA, McArdle JJ, Braun AR. Strategies for longitudinal
698 neuroimaging studies of overt language production. *Neuroimage*. 2009 Aug 15;47(2):745-55.
- 699 [54] Shehzad Z, Kelly AC, Reiss PT, Gee DG, Gotimer K, Uddin LQ, Lee SH, Margulies DS, Roy AK,
700 Biswal BB, Petkova E. The resting brain: unconstrained yet reliable. *Cerebral cortex*. 2009 Feb
701 16;19(10):2209-29.
- 702 [55] Zhao J, Liu J, Jiang X, Zhou G, Chen G, Ding XP, Fu G, Lee K. Linking resting-state networks in
703 the prefrontal cortex to executive function: a functional near infrared spectroscopy study. *Frontiers in*
704 *neuroscience*. 2016 Oct 7;10:452.
- 705
706
707
708
709
710



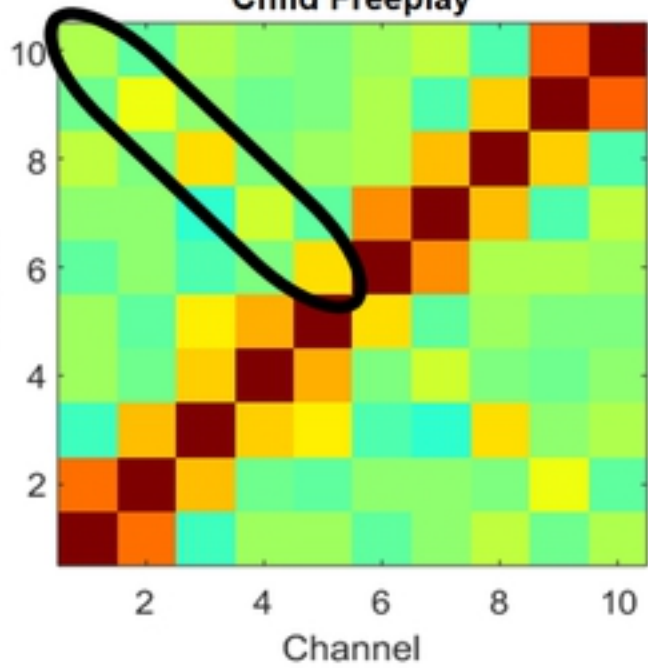




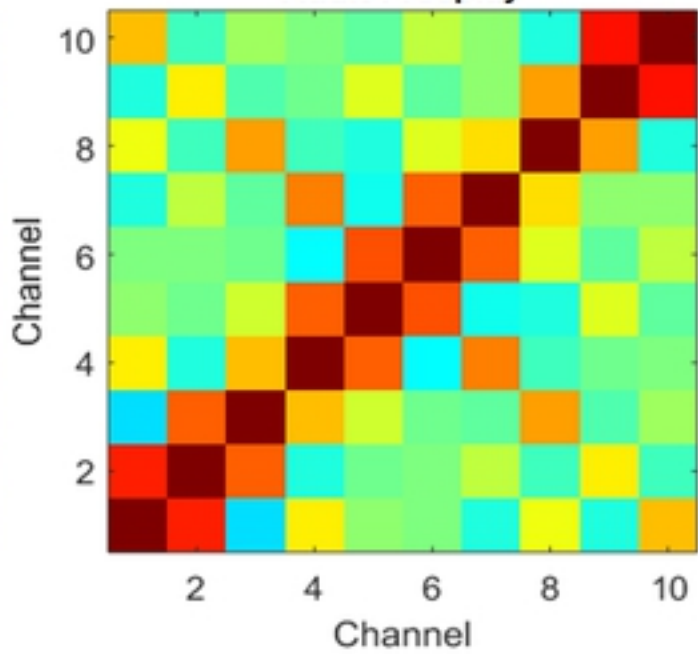




Child Freeplay



Adult Freeplay



Adult "at rest"

